A nonlinear beam finite element for curved and twisted composite helicopter blade

Yan Skladanek, Paul Cranga, Guy Ferraris, Georges Jacquet-Richardet, Régis Dufour

Paper number 065

A NONLINEAR BEAM FINITE ELEMENT FOR CURVED AND TWISTED COMPOSITE HELICOPTER BLADE

Yan Skladanek[1,2,3], Paul Cranga[1], Guy Ferraris[2], Georges Jacquet[2], Régis Dufour[2]

[1]*EUROCOPTER* – Dynamics Department, *13725 Marignane Cedex France*
[2]*Université de Lyon, CNRS, INSA-Lyon, LaMCoS UMR5259, F-69621, Villeurbanne, France*
[3]*Corresponding author: yan.skladanek@eurocopter.com*

ABSTRACT

Structural, shape and performances optimization in helicopter rotor leads to design composite blades initially curved and twisted. This design yields a highly coupled behavior between torsion, longitudinal and bending motions of blades. A non-linear Timoshenko-like straight beam finite element is proposed to predict the static deformation under aerodynamic and centrifugal loads and achieve dynamic and stability analysis. This elastic model is to be implemented in a comprehensive rotorcraft analysis code, which means accuracy, reliability and calculation time compromise. Model validation is based on analytical and numerical investigations. The developed model reveals to be very accurate for beams with extreme shapes compared to blade design. It is now expected to improve prediction quality for full helicopter simulation tools and particularly for rotor dynamic analysis.

Keywords: Timoshenko's beam, finite element, nonlinear, composite blade, shear locking free, rotational effects.

1. INTRODUCTION

Blade elastic behavior modeling is an important research topic for improvement of comprehensive rotorcraft analysis codes especially for dynamic and stability analysis, vibratory loads and performance calculations. The use of composite materials and new shapes for blades such as swept tip or evolutionary twist lead to study and develop beam theories in order to properly model both structural coupling phenomena and rotational effects.

Many efforts have been done to limit approximations when writing the equations of motion for rotating beams with arbitrary cross-sections. Early works [2],[3] introduced twist effects and coupling between bending and torsion motions. Ferraris' study on homogeneous cross-section [1] in the field of turbo machinery blade modeling makes clearly appear all coupling terms due to gravity and shear center non coincidence and adds to it twist dependency, geometrical non-linearity and rotational effects. Equations are obtained using Hamilton principle applied to strain and kinetics energies explicitly derived from beam fibers axial elongation. Hodges is one of the first to use a so-called "exact" method for helicopter blade modeling [4]. His work is widely used since then for composite blade modeling [11], [13], cross-sectional characteristics calculation [12], and comprehensive analysis codes assessment [6]. In those studies, both shear and warping effects are taken into account for equations development. Some other authors are particularly interested in initially curved beam, among them Borri and al. [14] and Geradin and al. [15]. Since helicopter blades can be considered as thin walled composite beams, Librescu and al. [16] give some elements in this way.

Numerical implementation of calculated equations is mainly achieved using Finite Element Method (FEM). For classical dynamic purpose, FEM is convenient and quite accurate if one pays attention to finite element capabilities. Another current method relies on dynamic stiffness matrix derived from frequency-dependant shape functions cutting down the number of elements needed. This method is often called Spectral Finite Element Method (SFEM) in literature. Chandrashekhara and al. [17] Banerjee and al. [19] or Mahapatra and al. [18] developed more and more complete models, all based on Wittrick and Williams algorithm [20] for natural frequency calculation.

As the beam elastic model developed in this paper is to be implemented in a comprehensive analysis code, FEM is retained, blades being meshed anyway for aerodynamic purpose. Regarding for full rotational capable elements, one can refer to Lalanne and Ferraris' book [5] both for rotating and fixed frame. Early work of Przemieniecki [7] introduced Timoshenko's shear coefficient [21] [22] in both stiffness and mass elementary matrix. Batoz and Dhatt [9] give a global view of beam finite element modeling undergoing many effects. The main contribution of our work is the introduction of shear effect in all matrices, including geometrical stiffness matrix and centrifugal force work. Moreover, an eight-degree-of-freedom per node finite element based on cubical shape functions is developed to increase convergence speed and avoiding shear locking effect [8]. Full multi-material cross-section capability is also added to [1]. At last, large displacement capability is provided to the finite element using co-rotational formulation from Criesfield work [10]. This element should fit all requirements for composite curved and twisted blade for articulated and rigid helicopter hubs.

2. EQUATIONS OF MOTION

Beam equations of motion are based on explicit writing of fibers axial elongation and velocity field as it is done in [1]. This method permits an exact development of strain and velocity fields, approximated by a second order scheme which leads to non-linear equations. Neutral fiber is taken as the reference axis for beam deformation, implying that without shear cross-sections initially perpendicular to this axis remain undeformed when small deformations are applied. Pure torsion motion is supposed to be uncoupled from bending and longitudinal motions, with this assumption it can be applied separately to the beam.

2.1 BEAM STRAIN FIELD

In beam theory, the effect of the strain field is limited to fibers axial elongation and torsion angle, e.g. to 1 dimension even if the beam is curved or twisted in space. One can deduce strain energy by knowing how beams fibers are stretched. First step consists in calculating fibers length before strain field is applied.

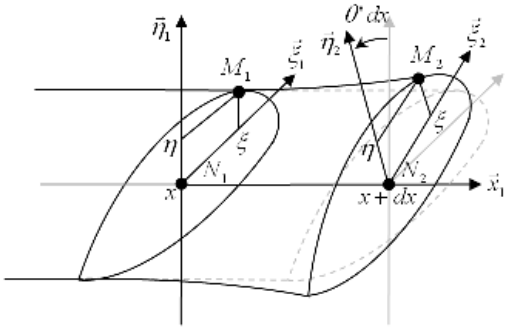

Figure 1 : Length of an undeformed fiber of the beam

For a short piece of beam, considered straight, with a length dx between the elastic centers N_1 and N_2 of its two extreme sections, the length of an unspecified fiber M_1M_2 is related to the initial twist angle per length unit θ' by :

$$\left|\overrightarrow{M_1M_2}\right| = \left(1+\frac{1}{2}(\eta^2+\xi^2)\theta'^2\right)dx \qquad (1)$$

Let us now consider the displacement field for one of the beam cross-section.

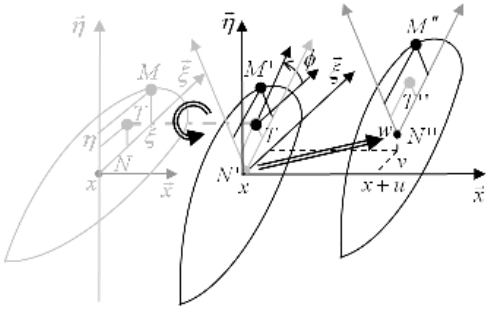

Figure 2 : Decomposition of beam deformation

First all points in the cross-section undergo torsion motion turning by a twist angle ϕ around the shear center T . Then longitudinal motion u and bending motions v and w are applied.

Considering a point M of the initial cross-section, M' is its counterpart after torsion motion and M'' its counterpart after bending and axial motions.

M and T are simply linked by their coordinate in initial frame $R = \left\langle N, \vec{x}, \vec{\xi}, \vec{\eta} \right\rangle$

$$\overrightarrow{TM} = \begin{Bmatrix} 0 \\ \xi - \xi_T \\ \eta - \eta_T \end{Bmatrix}_R \qquad (2)$$

By the same way M' and T are linked in the twisted frame, which give in R frame

$$\overrightarrow{TM'} = \begin{Bmatrix} 0 \\ (\xi-\xi_T)\cos\phi - (\eta-\eta_T)\sin\phi \\ (\eta-\eta_T)\cos\phi + (\xi-\xi_T)\sin\phi \end{Bmatrix}_R \qquad (3)$$

Introducing small bending angles ϕ_ξ around $\vec{\xi}$ and ϕ_η around $\vec{\eta}$, one can retrieve the link between M' and M''

$$\overrightarrow{M'M''} = \begin{Bmatrix} u + \eta_{M'}\phi_\xi - \xi_{M'}\phi_\eta \\ v \\ w \end{Bmatrix}_R \qquad (4)$$

with $\eta_{M'}$ and $\xi_{M'}$ the coordinates of M' in R frame.

The length of the fiber M_1M_2 after all motions being applied to cross-sections can be deduced from equations (1) to (4) by decomposing the vector $\overrightarrow{M_1''M_2''}$.

$$\begin{aligned}\overrightarrow{M_1''M_2''} = {} & \overrightarrow{M_1''M_1'} + \overrightarrow{M_1'T_1} + \overrightarrow{T_1M_1} \\ & + \overrightarrow{M_1M_2} \\ & + \overrightarrow{M_2T_2} + \overrightarrow{T_2M_2'} + \overrightarrow{M_2'M_2''}\end{aligned} \qquad (5)$$

Finally axial elongation of beam fibers can be simply expressed as :

$$\varepsilon = \frac{\left|\overrightarrow{M_1''M_2''}\right| - \left|\overrightarrow{M_1M_2}\right|}{\left|\overrightarrow{M_1M_2}\right|} \qquad (6)$$

Keeping in second order terms, the strain field within cross-section contains non-linear terms coupling each motion with all other.

$$\varepsilon = \varepsilon_l + \varepsilon_{nl} \qquad (7)$$

$$\varepsilon_l = u' - \xi\phi_\eta' + \eta\phi_\xi' + k\theta'\phi' \qquad (8)$$

$$\begin{aligned}\varepsilon_{nl} = {} & \frac{u'^2}{2} + \frac{v'^2}{2} + \frac{w'^2}{2} + \frac{\phi_\eta^2}{2}\eta^2\theta'^2 + \frac{\phi_\xi^2}{2}\xi^2\theta'^2 + h\phi'^2 \\ & + \xi^2\frac{\phi_\eta'^2}{2} + \eta^2\frac{\phi_\xi'^2}{2} \\ & + (\xi-\xi_T)x\phi_\xi'\phi' + (\eta-\eta_T)x\phi_\eta'\phi' \\ & + \xi\theta'u'\phi_\xi + \eta\theta'u'\phi_\eta + \eta u'\phi_\xi' - \xi u'\phi_\eta' \\ & + \xi\eta\theta'\phi_\xi\phi_\xi' - \xi\eta\theta'\phi_\eta\phi_\eta' + \xi\eta\theta'^2\phi_\eta\phi_\xi - \xi\eta\phi_\eta'\phi_\xi' \\ & - \xi^2\theta'\phi_\eta'\phi_\xi + \eta^2\theta'\phi_\eta\phi_\xi'\end{aligned} \qquad (9)$$

with k and h two constants depending on points coordinates and using $(\,)' = \frac{d}{dx}$

In addition, Timoshenko's beam theory is used to link bending angles to lateral displacement:

$$\phi_\eta = v' + C_\xi \tag{10}$$

$$\phi_\xi = -w' + C_\eta \tag{11}$$

2.2 BEAM VELOCITY FIELD

To introduce rotational effects in the velocity field of the beam, consider the fixed frame $R_0 = \langle O, \vec{X}, \vec{Y}, \vec{Z} \rangle$. Beam is rotating around $\vec{Z}$ at a speed of Ω. Position of a point M_1 after application of the displacement field is decomposed as:

$$\overrightarrow{OM_1}'' = \overrightarrow{ON} + \overrightarrow{NN_1} + \overrightarrow{N_1T_1} + \overrightarrow{T_1M_1}' + \overrightarrow{M_1'M_1}'' \tag{12}$$

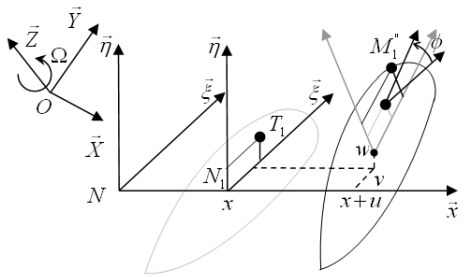

Figure 3 : Cross-section displacement field

Beam is considered as straight between a first cross-section of elastic center N and the current cross-section. Point O coordinates in R frame is $\langle x_A, \xi_A, \eta_A \rangle$. Using expressions (3) and (4), one can find :

$$\overrightarrow{OM_1}'' = \begin{Bmatrix} x_A + x + u + (\eta + (\xi - \xi_t)\phi)\phi_\xi - (\xi - (\eta - \eta_t)\phi)\phi_\eta \\ \xi_A + \xi + v - (\eta - \eta_t)\phi \\ \eta_A + \eta + w + (\xi - \xi_t)\phi \end{Bmatrix}_R \tag{13}$$

Velocity of point M_1 in the rotating frame R is then:

$$\overrightarrow{V_{M_1}} = \frac{\overrightarrow{\partial OM_1}''}{\partial t} + \overrightarrow{\Omega_{R1/R0}} \Lambda \overrightarrow{OM_1}'' \tag{14}$$

Using $\dot{(\,)} = \frac{d}{dt}$, we have :

$$\frac{\overrightarrow{\partial OM_1}''}{\partial t} = \begin{Bmatrix} \dot{u} + \eta\dot{\phi}_\xi - \xi\dot{\phi}_\eta \\ \dot{v} - (\eta - \eta_t)\dot{\phi} \\ \dot{w} + (\xi - \xi_t)\dot{\phi} \end{Bmatrix}_R \tag{15}$$

and

$$\overrightarrow{\Omega_{R1/R0}} = \begin{Bmatrix} \Omega_1 \\ \Omega_2 \\ \Omega_3 \end{Bmatrix}_R \tag{16}$$

the rotational vector expressed in R frame.

2.3 LAGRANGE'S EQUATIONS

Applying Lagrange's equations to the strain and kinetic energies is a very common way to determine equations of motion using Hamilton's principle. Without damping and external forces other than centrifugal forces, equations are:

$$\frac{d}{dt}\left(\frac{dT}{d\dot{q}_i}\right) - \frac{dT}{dq_i} + \frac{dU}{dq_i} = 0 \tag{17}$$

q_i : generalized coordinates,

T : kinetic energy, U : strain energy.

2.3.1 STRAIN ENERGY

Strain energy can be deduced from strain field all along the beam by adding to it the pure torsion strain energy:

$$U = U_L + U_T \tag{18}$$

Torsion energy is classically:

$$U_T = \frac{1}{2}\int_L GJ_T\phi'^2 dx \tag{19}$$

with J_T the cross-section torsion constant, G its shear modulus and L the beam length.

Strain energy due to beam elongation is :

$$U_L = \frac{1}{2}\int_V E\varepsilon^2 dV \tag{19}$$

with E the Young modulus of the cross-section.

Equation (19) is developed in details by the introduction of the non-linearity of the elongation stressed in equation (7) and of the shear energy resulting from beam deformation.

$$U_L = U_{l-l} + U_{l-nl} + U_{nl-nl} + U_{shear} \tag{20}$$

One can retrieve classical linear strain energy:

$$U_{l-l} = \frac{1}{2}\int_V E\varepsilon_l^2 dV \tag{21}$$

Shear energy results from introduction of Timoshenko's theory in eq. (10) and (11) when linking bending angles to lateral displacements:

$$U_{shear} = \frac{1}{2}\int_V (2\sigma_{x\xi}\varepsilon_{x\xi} + 2\sigma_{x\eta}\varepsilon_{x\eta})dV \tag{22}$$

with

$$2\varepsilon_{x\xi} = -\phi_\eta + v' \tag{23}$$

$$2\varepsilon_{x\eta} = \phi_\xi + w' \tag{24}$$

Introducing k_ξ and k_η, the Timoshenko's shear coefficients for each bending axis defined as:

$$\frac{T_\xi{}^2}{k_\xi S} = \int \sigma_{x\xi} dS \quad , \qquad \frac{T_\eta{}^2}{k_\eta S} = \int \sigma_{x\eta} dS \qquad (25), (26)$$

with T_ξ and T_η transverse forces applied to the cross-section and S its area. kS represents the sheared area also often called "reduced section".

Transverse shear stresses are then:

$$\sigma_{x\xi} = 2Gk_\xi \varepsilon_{x\xi} \qquad (27)$$

$$\sigma_{x\eta} = 2Gk_\eta \varepsilon_{x\eta} \qquad (28)$$

From which one can get:

$$U_{shear} = \frac{1}{2}\int_V 4G(k_\xi \varepsilon_{x\xi}^2 + k_\eta \varepsilon_{x\eta}^2))dV \qquad (29)$$

Non-linear terms give:

$$U_{l-nl} = \int_V E\varepsilon_l \varepsilon_{nl} dV = \int_V \sigma_0 \varepsilon_{nl} dV \qquad (30)$$

with σ_0 the initial axial stress within the beam.

At last remaining terms can be neglected as cross products between non-linear terms are high order terms.

$$U_{nl-nl} = \frac{1}{2}\int_V E\varepsilon_{nl}^2 dV \qquad (31)$$

2.3.2 KINETIC ENERGY

Kinetic energy is directly calculated from the velocity field along the beam:

$$T = \frac{1}{2}\int_V \rho V_M{}^2 dV \qquad (32)$$

with ρ the density of the cross-section.

Kinetic energy terms can be gathered depending on their order and their derivation with respect to time. 2nd order "velocity" terms lead to define a mass matrix. A stiffness matrix can be built with 2nd order "displacement" terms, while cross products between velocity and displacement terms make appear the gyroscopic matrix. At last first order "displacement" terms correspond to centrifugal force work. Other terms disappear when Lagranges' equations are applied.

$$T = T_{mass} + T_{stiff} + T_{gyro} + T_{cf} + T_{other} \qquad (33)$$

2.3.3 MATRIX FORM OF EQUATIONS

Introducing results from (21),(29),(30) and (32) in equation (17) the final equations of motion governing the rotating beam movements can be formed.

$$M\ddot{q} + C(\Omega)\dot{q} + \left(K + K_G(\sigma_0) - K_S(\Omega^2)\right)q = F_C(\Omega^2) + F_{ext} \qquad (34)$$

Conveniently the matrix form of the equations makes appear classical mass and stiffness matrices but also some other terms detailed here after.

M : Mass matrix, including rotatory inertia
C : Gyroscopic matrix (Coriolis effect)
K : Stiffness matrix, including shear stiffness and pure torsion stiffness
K_G : Stress stiffening matrix (making equations nonlinear)
K_S : Spin softening matrix
F_C : Centrifugal force
F_{ext} : Other external forces

3. FINITE ELEMENT DEFINITION

The finite element proposed in this paper is an advanced beam element, undergoing shear effects without shear locking, having non-classical degrees of freedom to reduce the number of elements needed, and being compliant with multi-body numerical methods requirements.

3.1 SHAPE FUNCTIONS

The choice of shape functions is one of the main issues when formulating a finite element, conditioning Degrees of Freedom (DoF) that will be included in the model, and the accuracy of results.

Classical cubical shape functions are chosen for lateral displacements in order to link corresponding bending angles (eq. 10 and 11).

$$v(x) = a_5 + a_6 x + a_7 x^2 + a_8 x^3 \qquad (35)$$

$$w(x) = a_9 + a_{10} x + a_{11} x^2 + a_{12} x^3 \qquad (36)$$

The innovation of our work is to choose again cubical shape functions for longitudinal displacement and torsion motion.

$$u(x) = a_1 + a_2 x + a_3 x^2 + a_4 x^3 \qquad (37)$$

$$\phi(x) = a_{13} + a_{14} x + a_{15} x^2 + a_{16} x^3 \qquad (38)$$

These shape functions involve the inclusion of longitudinal and torsion motions derivatives in the element DoF. This permits not to assemble these derivatives of two successive elements, e.g. to let them free. Doing this, one can ensure torque and longitudinal load transmission between two elements with different cross sectional

characteristics, with no need for a mesh refinement around the transition zone.

A simple example (fig. 4) can exhibit the interest of such a choice. Torsion momentum is related to the torsion angle through the cross-sectional inertia and material properties:

$$M_1 = E_1 I_1 \frac{\partial \phi_1}{\partial x} \quad , \quad M_2 = E_2 I_2 \frac{\partial \phi_2}{\partial x} \qquad (39),(40)$$

Torque is to be transmitted from element 1 to element 2. Elements have different cross-sections at their common node and are possibly made of different materials:

$$M_1 = M_2 \quad , \quad E_1 I_1 \neq E_2 I_2 \qquad (41),(42)$$

$$\frac{\partial \phi_1}{\partial x} \neq \frac{\partial \phi_2}{\partial x} \qquad (43)$$

Eq. (39), (40) and (42) imply from (41) that torsion angle derivatives for both element remain free, which cannot be ensured if these derivatives are not permitted DoF of the finite element. Same demonstration can be performed for longitudinal load transmission.

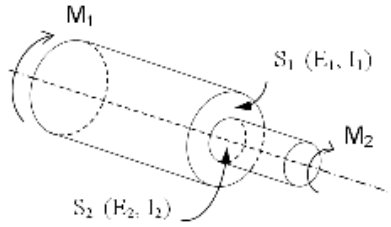

Figure 4 : Torque transmission between two different elements

3.2 DEGREES OF FREEDOM

Considering now a single node of one beam element, the minimum number of independent DoF is half the number of unknowns in shape functions (35)-(38). As for classical 3D beam finite elements, 6 DoF are chosen to locate the node in space. Derivatives of longitudinal displacement and torsion motion are added. In order not to assemble those 2 DoF between two elements, each node has to separate contributions coming from left-side element and right-side element (resp. *l* and *r* subscripts).

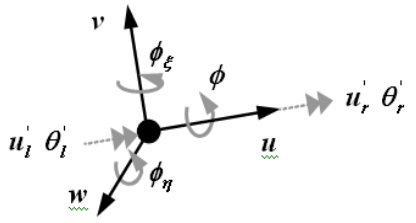

Figure 5 : Beam element node degrees of freedom

Finally each node has 10 attached DoF, which means 20 DoF for one beam element:

$$\langle \delta_N \rangle = \langle u_1, v_1, w_1, \phi_1, \phi_{\xi 1}, \phi_{\eta 1}, u'_{1g}, u'_{1d}, \phi'_{1g}, \phi'_{1d}, u_2, v_2, w_2, \phi_2, \phi_{\xi 2}, \phi_{\eta 2}, u'_{2g}, u'_{2d}, \phi'_{2g}, \phi'_{2d} \rangle \qquad (44)$$

Shape functions coefficients a_1 to a_{16} are related to DoF by matrix A :

$$\begin{Bmatrix} a_1 \\ a_2 \\ \vdots \\ a_{16} \end{Bmatrix} = [A]\{\delta_N\} \qquad (45)$$

Coefficients of equations (37) and (38) are easily found using element boundary conditions for longitudinal and torsion motions.

$$u(0) = u_1 \,,\; u(L) = u_2 \qquad (46)$$

$$u'(0) = u'_{1d} \,,\; u'(L) = u'_{2g} \qquad (47)$$

$$\phi(0) = \phi_1 \,,\; \phi(L) = \phi_2 \qquad (48)$$

$$\phi'(0) = \phi'_{1d} \,,\; \phi'(L) = \phi'_{2g} \qquad (49)$$

with L the element length.

For bending motions, shear effects have to be added in order to correctly derive shape functions coefficients.

3.3 INTRODUCTION OF SHEAR

Transverse shear effects modify the beam behavior in bending motions, adding cross-section rotations to ones produced by lateral displacements. Those displacements and bending angles are cinematically linked together trough eq. (10) and (11) with Timoshenko's theory. Developing this relation between DoF, one can build a finite element free from shear locking as explained in [8].

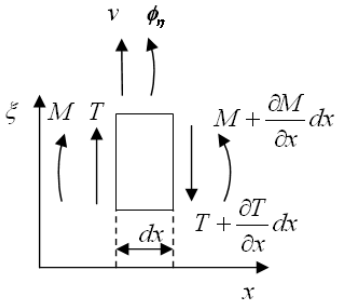

Figure 6 : Beam equilibrium

Let's consider only one bending motion. Fig. 6 exhibits how forces and momentum are balanced within a short part of the beam. Eq. (23), (25) and (27) can be combined to retrieve classical relation between shear transverse force and Timoshenko's supplementary shear rotation of cross-section (Eq. 10).

$$T = C_\xi k_\xi S G \qquad (50)$$

From static equilibrium we have:

$$\frac{\partial T}{\partial x} = 0 \quad , \quad \frac{\partial M}{\partial x} = T \qquad (51), (52)$$

From theory of strength of materials we have:

$$\frac{\partial \phi_\eta}{\partial x} = \frac{M}{EI} \qquad (53)$$

Deriving eq. (10) gives:

$$\frac{\partial^2 \phi_\eta}{\partial x^2} = \frac{\partial^3 v}{\partial x^3} \tag{54}$$

Eventually eq. (50) to (54) lead to

$$C_\xi = \frac{EI}{k_\xi G}\frac{\partial^3 v}{\partial x^3} \tag{55}$$

As for longitudinal displacement and torsion angle, shape function coefficients are deduced from boundary conditions at element ends applied to eq. (35) with relations (10) and (55) between DoF.

$$v(0) = v_1,\ v(L) = v_2,\ \phi_\eta(0) = \phi_{\eta 1} \text{ et } \phi_\eta(L) = \phi_{\eta 2} \tag{56}$$

$$\frac{\partial v}{\partial x} = a_6 + 2a_7 x + 3a_8 x^2 = \phi_\eta - C_\xi \tag{57}$$

$$\frac{\partial^3 v}{\partial x^3} = 6a_8 \Rightarrow C_\xi = \frac{L^2 a_\xi}{2} a_8 \tag{58}$$

with $a_\xi = \dfrac{12EI}{Gk_\xi SL^2}$ the shear coefficient introduced by [7], conveniently being almost null for long slender beams for which shear effects can be neglected.

As shear effects is being included in shape functions, all matrices will be shear dependant. This ensures that shear is fully represented by the formulated finite element.

3.4 MATRICES IN LOCAL ELEMENT FRAME

Matrices used in eq. (34) are directly formed by application of Lagranges' equations on kinetic and strain energies. For each element, non-integrated elementary matrices are calculated in local frame, using generalized DoF and their derivatives. All matrices presented here should be integrated over cross-sections and along the element. It can be expressed relatively to element DoF frame with eq. (44) and (45).

3.4.1 STIFFNESS MATRIX

Classical stiffness matrix is derived from linear terms of strain energy (including pure torsion terms):

$$U_{l-l} + U_T = \frac{1}{2}\int_V \langle \delta_c \rangle [K_{cg}] \{\delta_c\} dV \tag{59}$$

where generalized DoF vector is

$$\langle \delta_c \rangle = \langle u', v'', w'', \phi' \rangle \tag{60}$$

Non-integrated symmetrical stiffness matrix is then:

$$[K_{cg}] = E\begin{bmatrix} 1 & -\xi & -\eta & k\theta' \\ & \xi^2 & \eta\xi & -\xi k\theta' \\ Sym. & & \eta^2 & -\eta k\theta' \\ & & & k^2\theta'^2 + \dfrac{GJ_T}{S} \end{bmatrix} \tag{61}$$

3.4.2 SHEAR STIFFNESS MATRIX

Shear effects result in an additional stiffness matrix coming from eq. (29) considering relation (55).

$$U_{shear} = \frac{1}{2}\int_V \langle \delta_{shear} \rangle [K_{she\arg}] \{\delta_{shear}\} dV \tag{62}$$

$$\langle \delta_{shear} \rangle = \langle v''', w''' \rangle \tag{63}$$

$$[K_{she\arg}] = E\begin{bmatrix} \dfrac{\xi^2 L^2 a_\xi}{12} & 0 \\ 0 & \dfrac{\eta^2 L^2 a_\eta}{12} \end{bmatrix} \tag{64}$$

3.4.3 STRESS STIFFNESS MATRIX

Stress stiffness matrix can be calculated once the mean axial stress is computed:

$$U_{l-nl} = \frac{1}{2}\sigma_0 \int_V \langle \delta_g \rangle [K_{gg}] \{\delta_g\} dV \tag{65}$$

$$\langle \delta_g \rangle = \langle u', v', w', v'', w'', v''', w''', \phi' \rangle \tag{66}$$

$$[K_{gg}] = \begin{bmatrix} 1 & \eta\theta' & -\xi\theta' & -\xi & -\eta & \dfrac{\eta\theta' L^2 a_\xi}{12} & \dfrac{-\xi\theta' L^2 a_\eta}{12} & 0 \\ & 1+\eta^2\theta'^2 & -\xi\eta\theta'^2 & -\xi\eta\theta' & -\eta^2\theta' & \dfrac{\eta^2\theta'^2 L^2 a_\xi}{12} & \dfrac{-\xi\eta\theta'^2 L^2 a_\eta}{12} & 0 \\ & & 1+\xi^2\theta'^2 & \xi^2\theta' & \xi\eta\theta' & \dfrac{-\xi\eta\theta'^2 L^2 a_\xi}{12} & \dfrac{\xi^2\theta'^2 L^2 a_\eta}{12} & 0 \\ & & & \xi^2 & \xi\eta & \dfrac{-\xi\eta\theta' L^2 a_\xi}{12} & \dfrac{\xi^2\theta' L^2 a_\eta}{12} & (\eta-\eta_t)x \\ & & & & \eta^2 & \dfrac{-\eta^2\theta' L^2 a_\xi}{12} & \dfrac{\xi\eta\theta' L^2 a_\eta}{12} & -(\xi-\xi_t)x \\ & & & & & \dfrac{\eta^2\theta'^2 L^4 a_\xi^2}{144} & \dfrac{-\xi\eta\theta'^2 L^4 a_\xi a_\eta}{144} & 0 \\ & Sym. & & & & & \dfrac{\xi^2\theta'^2 L^4 a_\eta^2}{144} & 0 \\ & & & & & & & 2h \end{bmatrix} \tag{67}$$

3.4.4 MASS MATRIX

Mass matrix, including rotatory inertia effects, comes from kinetic energy 2nd order "velocity" terms.

$$T_{mass} = \frac{1}{2}\int_V \langle \dot{\delta}_m \rangle [M_g] \{\dot{\delta}_m\} dV \tag{68}$$

$$\langle \dot{\delta}_m \rangle = \langle \dot{u}, \dot{v}, \dot{w}, \dot{v}', \dot{w}', \dot{v}''', \dot{w}''', \dot{\phi} \rangle \tag{69}$$

$$[M_g] = \rho\begin{bmatrix} 1 & 0 & 0 & -\xi & -\eta & -\dfrac{\xi L^2 a_\xi}{12} & -\dfrac{\eta L^2 a_\eta}{12} & 0 \\ & 1 & 0 & 0 & 0 & 0 & 0 & -(\eta-\eta_t) \\ & & 1 & 0 & 0 & 0 & 0 & (\xi-\xi_t) \\ & & & \xi^2 & \xi\eta & \dfrac{\xi^2 L^2 a_\xi}{12} & \dfrac{\xi\eta L^2 a_\eta}{12} & 0 \\ & & & & \eta^2 & \dfrac{\xi\eta L^2 a_\xi}{12} & \dfrac{\eta^2 L^2 a_\eta}{12} & 0 \\ & & & & & \dfrac{\xi^2 L^4 a_\xi^2}{144} & \dfrac{\xi\eta L^4 a_\xi a_\eta}{144} & 0 \\ & Sym. & & & & & \dfrac{\eta^2 L^4 a_\eta^2}{144} & 0 \\ & & & & & & & I_T \end{bmatrix} \tag{70}$$

with $I_T = (\xi-\xi_t)^2 + (\eta-\eta_t)^2$

3.4.5 SUPPLEMENTARY STIFFNESS MATRIX

Doing the same for 2nd order "displacement" terms, the supplementary stiffness matrix can be found:

$$T_{stiff} = \frac{1}{2}\int_V \langle \dot{\delta}_s \rangle [K_{sg}] \{\dot{\delta}_s\} dV \tag{68}$$

$$\langle \delta_s \rangle = \langle u, v, w, v', w', v''', w''', \phi \rangle \tag{69}$$

$$[K_{sg}] = -\rho \begin{bmatrix} A & -\gamma & -\beta & -\xi A & -\eta A & \frac{-L^2\xi a_\xi}{12}A & \frac{-L^2\eta a_\eta}{12}A & (\eta-\eta_t)\gamma-(\xi-\xi_t)\beta \\ & B & -\alpha & \xi\gamma & \eta\gamma & \frac{L^2\xi a_\xi}{12}\gamma & \frac{L^2\eta a_\eta}{12}\gamma & -(\eta-\eta_t)B-(\xi-\xi_t)\alpha \\ & & C & \xi\beta & \eta\beta & \frac{L^2\xi a_\xi}{12}\beta & \frac{L^2\eta a_\eta}{12}\beta & (\eta-\eta_t)\alpha+(\xi-\xi_t)C \\ & & & \xi^2 A & \xi\eta A & \frac{L^2\xi^2 a_\xi}{12}A & \frac{L^2\xi\eta a_\eta}{12}A & -\xi(\eta-\eta_t)\gamma+\xi(\xi-\xi_t)\beta \\ & & & & \eta^2 A & \frac{L^2\xi\eta a_\xi}{12}A & \frac{L^2\eta^2 a_\eta}{12}A & -\eta(\eta-\eta_t)\gamma+\eta(\xi-\xi_t)\beta \\ & & & & & \frac{L^4\xi^2 a_\xi^2}{144}A & \frac{L^4\xi\eta a_\xi a_\eta}{144}A & (-\xi(\eta-\eta_t)\gamma+\xi(\xi-\xi_t))\beta\frac{L^2 a_\xi}{12} \\ & Sym. & & & & & \frac{L^4\eta^2 a_\eta^2}{144}A & (-\eta(\eta-\eta_t)\gamma+\eta(\xi-\xi_t)\beta)\frac{L^2 a_\eta}{12} \\ & & & & & & & D \end{bmatrix} \tag{70}$$

with $A = \Omega_2{}^2 + \Omega_3{}^2$, $B = \Omega_1{}^2 + \Omega_3{}^2$, $C = \Omega_1{}^2 + \Omega_2{}^2$,

$\alpha = \Omega_2\Omega_3$, $\beta = \Omega_1\Omega_3$, $\gamma = \Omega_1\Omega_2$,

$$D = \left(\Omega_2(\xi-\xi_t)+\Omega_3(\eta-\eta_t)\right)^2 + \Omega_1{}^2\left((\xi-\xi_t)^2+(\eta-\eta_t)^2\right)$$
$$= C(\xi-\xi_t)^2 + B(\eta-\eta_t)^2 + 2\alpha(\xi-\xi_t)(\eta-\eta_t)$$

3.4.6 GYROSCOPIC MATRIX

Damping-like terms lead to the gyroscopic matrix:

$$T_{gyro} = \int_V \langle \delta_c \rangle [C_g] \{\dot{\delta}_c\} dV, \qquad \langle \delta_c \rangle = \langle \delta_s \rangle \tag{71), (72}$$

$$[C_g] = -2\rho \begin{bmatrix} 0 & \Omega_3 & -\Omega_2 & 0 & 0 & 0 & 0 & -\Omega_3(\eta-\eta_t) \\ & 0 & \Omega_1 & \Omega_3\xi & \Omega_3\eta & \frac{L^2 a_\xi}{12}\Omega_3\xi & \frac{L^2 a_\eta}{12}\Omega_3\eta & -\Omega_2(\xi-\xi_t) \\ & & 0 & -\Omega_2\xi & -\Omega_2\eta & \frac{-L^2 a_\xi}{12}\Omega_2\xi & \frac{-L^2 a_\eta}{12}\Omega_2\eta & \Omega_1(\xi-\xi_t) \\ & & & 0 & 0 & 0 & 0 & \Omega_1(\eta-\eta_t) \\ & & & & 0 & 0 & 0 & \Omega_3\xi(\eta-\eta_t) \\ & & & & & 0 & 0 & +\Omega_2\xi(\xi-\xi_t) \\ & & & & & & 0 & \Omega_3\eta(\eta-\eta_t) \\ & & & & & & & +\Omega_2\eta(\xi-\xi_t) \\ & & & & & 0 & 0 & \frac{L^2 a_\xi}{12}\begin{pmatrix}\Omega_3\xi(\eta-\eta_t) \\ +\Omega_2\xi(\xi-\xi_t)\end{pmatrix} \\ & AntiSym. & & & & & 0 & \frac{L^2 a_\eta}{12}\begin{pmatrix}\Omega_3\eta(\eta-\eta_t) \\ +\Omega_2\eta(\xi-\xi_t)\end{pmatrix} \\ & & & & & & & 0 \end{bmatrix} \tag{73}$$

3.4.7 CENTRIFUGAL FORCE VECTOR

At last, centrifugal forces are deduced from remaining terms:

$$T_{cf} = \int_V \langle F_{cg} \rangle \{\dot{\delta}_{cf}\} dV, \qquad \langle \delta_{cf} \rangle = \langle \delta_s \rangle \tag{74), (75}$$

$$\{F_{cg}\} = \rho \begin{Bmatrix} A(x_A+x)-\beta(\eta_A+\eta)-\gamma(\xi_A+\xi) \\ B(\xi_A+\xi)-\alpha(\eta_A+\eta)-\gamma(x_A+x) \\ C(\eta_A+\eta)-\beta(x_A+x)-\alpha(\xi_A+\xi) \\ -A\xi(x_A+x)+\beta\xi(\eta_A+\eta)+\gamma\xi(\xi_A+\xi) \\ -A\eta(x_A+x)+\beta\eta(\eta_A+\eta)+\gamma\eta(\xi_A+\xi) \\ \frac{L^2 a_\xi}{12}\left(-A\xi(x_A+x)+\beta\xi(\eta_A+\eta)+\gamma\xi(\xi_A+\xi)\right) \\ \frac{L^2 a_\eta}{12}\left(-A\eta(x_A+x)+\beta\eta(\eta_A+\eta)+\gamma\eta(\xi_A+\xi)\right) \\ \begin{vmatrix} -B\xi_A(\eta-\eta_t)+B\xi\eta_t+C\eta_A(\xi-\xi_t)-C\xi\eta_t \\ +E\eta\xi-\beta(x_A+x)(\xi-\xi_t)+\gamma(x_A+x)(\eta-\eta_t) \\ +\alpha[(\eta_A+\eta)(\eta-\eta_t)-(\xi_A+\xi)(\xi-\xi_t)] \end{vmatrix} \end{Bmatrix} \tag{76}$$

3.5 ELEMENTS ASSEMBLY

In order to assemble matrices coming from each element of the system, one has to express all this matrices in a unique reference frame, with common DoF between elements. For helicopter blades, the rotating frame attached to the rotor hub is chosen as a reference frame for pitch, flapping and lead-lag angles. Blades are articulated on the rotor hub (or can be considered articulated for rigid rotor hub), which means they can undergo large rotations in space.

The transformation matrix used is derived from Olindes-Rodrigues formula, using Tayt-Bryan like angles. Rotation of each element is obtained by applying successively flapping (β), lead-lag (δ) and pitch (θ) angles.

$$[M] = \begin{bmatrix} \cos\beta\cos\delta & -\cos\beta\cos\varphi\sin\delta+\sin\beta\sin\varphi & \cos\varphi\sin\beta+\cos\beta\sin\delta\sin\varphi \\ \sin\delta & \cos\delta\cos\varphi & -\cos\delta\sin\varphi \\ -\cos\delta\sin\beta & \cos\varphi\sin\beta\sin\delta+\cos\beta\sin\varphi & \cos\beta\cos\varphi-\sin\beta\sin\delta\sin\varphi \end{bmatrix}_{R_0} \tag{58}$$

3.6 MULTI-BODY NUMERICAL METHODS

As the finite element is to be included into a comprehensive rotorcraft analysis code to model articulated blades possibly connected to various other elements (e.g. lead lag dampers), it has to be compliant with multi-body numerical methods requirements. For static purpose large displacements must be permitted to find the equilibrium between external loads and interior efforts. The use of a reduced model is also needed as the trim calculation relies on a harmonic analysis of the blade dynamic modes.

Large displacement capability implies to update the blade position in space and its deformation during trim. Several approaches can be employed.

To evaluate the element the co-rotational formulation [10] is used as an enhancement of the finite element code programmed for test purpose. This method consists in 4 main steps. First deformation field is computed from external loads. Then the blade position is updated. Due to this new position the beam is abnormally stretched which leads to internal forces. The geometrical stiffness is then updated and the calculation returns to step 1, until an equilibrium position is found between external loads and internal forces.

In a comprehensive rotorcraft analysis code, rigid body motions are managed globally, and the blade model only needs to know the position of interfaces nodes, e.g. nodes that are connected to other model. At each step internal loads should be evaluated to correctly compute the centrifugal stiffness of the blade.

As the model is only seen by the comprehensive code by its interface nodes, it can be reduced using substructure techniques such as Craig and Bampton method [23]. This permits to reduce the number of degrees of freedom to be trimmed by the code.

4. NUMERICAL EXAMPLE

The presented finite element is implemented in MATLAB to assess the model capabilities. Model validation is based on analytical and numerical investigations. Several test beams are used to show separately the good implementation of each required effects to predict efficiently the real dynamic behavior of helicopter blades.

An acceptable model assessment requires controlling two main aspects of the test case: the data input for the developed beam model, and the 3D finite element model used to calculate reference results. This explains why a present blade can't be used to assess the model: composite twisted and curved blades are hard to model with 3D finite element and cross-section characteristics calculation uncertainties could distort results. Instead, one ideal test case is presented here to justify the capability of the developed finite element to model helicopter blades.

4.1 TWISTED AND CURVED BEAM

The test case is a curved and twisted homogeneous beam. Its neutral fiber describes a quadrant, with an important twist angle of 90 degrees at its tip. The cross-section is a half of disc which has its shear center off-set from the inertia center.

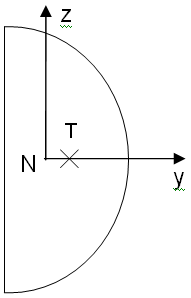

Figure 7 : Cross section

Beam characteristics :

Length : 1m
Diameter : 35mm
Twist angle : 90°
Young modulus : 2E11Pa
Poisson coef. : 0.3
Density : 7800kg/m^3
Shear coefficients :
ky=0.766 kz=0.863
Shear center offset : 3mm

This beam has a strong torsion-bending coupling behavior coming for both its shape and its shear center offset. Its characteristics are way more severe than those of any blade design. We assume that if the present finite element can model such a beam, it will be perfectly suited for blade modeling.

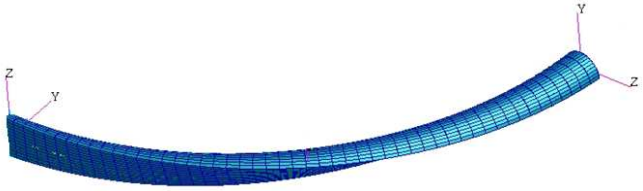

Figure 8 : Twisted and curved beam (NASTRAN)

The reference results are computed with NASTRAN 3D finite elements. HEX20 elements are chosen with 38 nodes to describe the cross-section contour and 50 elements spanwise. Only 40 elements were used for our 1D model.

First a modal analysis is performed without rotation to verify that the coupling is correctly modeled. Clamped – free boundary conditions are used. Results show that frequencies are very close to the reference calculation. Focusing on sixth mode, here reconstructed from the 1D results, one can appreciate the coupling behavior of the beam.

Table 1
Natural frequencies of the clamped-free beam at rest

Mode number	REF (Hz)	1D finite element (Hz)	Error (%)
1	28.4	28.0	-1.3
2	41.232	41.1	-0.4
3	154.0	152.4	-1.0
4	194.9	197.1	1.1
5	491.0	495.5	0.9
6	596.6	595.4	0.2
7	916.2	930.5	1.6
8	1011.1	1041	3.0
9	1215.5	1240.7	2.1
10	1680.5	1707.4	1.6

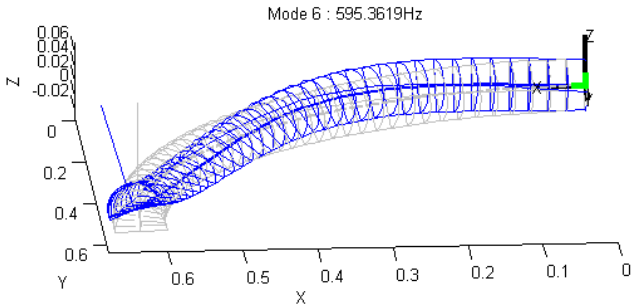

Figure 9 : Torsion-bending coupling on mode 6

Adding rotational effects with a rotation speed of 100 rad/s, another modal analysis is performed to demonstrate the good behaviour of the element under centrifugal loads.

Table 2
Natural frequencies of the clamped-free beam in rotation

Mode number	REF (Hz)	1D finite element (Hz)	Error (%)
1	29.4	29.1	-1.1
2	44.0	44.2	0.5
3	156.4	155.1	-0.8
4	195.9	200.1	2.1
5	493.6	498.9	1.1
6	599.2	602.6	0.5
7	923.7	931.1	0.8
8	1013.6	1044.5	3.1
9	1218.6	1244.0	2.1
10	1681.7	1708.4	1.6

Again the results show the good accuracy of the proposed model, with the same trends for the centrifugal stiffening and relative error remaining quite the same at rest or in rotation.

The finite element proves to be well suited to model curved and twisted beam having a strong coupling behavior which is the case for helicopter blades.

5. CONCLUSION

A nonlinear beam finite element is formulated in this paper to enhance helicopter blade modeling for comprehensive rotorcraft analysis codes.

First, governing equations were derived from an energetic approach, making assumptions compliant with blade characteristics such as twist or composite cross-sections. This step ensures keeping in the model all significant effects acting on the blades, especially inertia and rotating ones.

The novelty of this work comes from the numerical transcription of these equations, using the well-known finite element method with some extra features added to classical beam element. Shape functions are chosen to avoid shear locking and to reduce the number of elements needed. Those two issues are quite convenient for helicopter blade modeling. Shear can be neglected for static purpose but becomes important in dynamic analysis so that shear locking would have limited the use of the element, and a comprehensive code claims for a limited number of degrees of freedom for efficiency matters. Eventually, efforts were made to properly include in the element formulation all effects highlighted in the theoretical development: composite cross-sections, evolutionary twist, geometrical nonlinearity and rotational effects including gyroscopic and spin softening matrices.

The element capabilities have been investigated through numerical test cases in order to control the assessment process. The presented test case has exhibited the good behavior of the finite element for extreme curved and twisted beams validating though the element capability to model an actual helicopter blade with its geometrical specificities. Non-homogeneous cross-sections modeling is dependant of homogenization step, thus test cases using those multi-material sections should be related to the homogenization technique which is not the matter here. Those results need to be confirmed by experimentations; however numerical tests are very encouraging.

The proposed finite element should improve greatly present numerical blade models in comprehensive rotorcraft analysis codes as its formulation was designed for it, ensuring in particular the compliancy with multi-body requirements.

BIBLIOGRAPHY

[1] **FERRARIS-BESSO G.,** *Prévision du comportement dynamique des ensembles disque-aubes.* PhD. Lyon: INSA de Lyon, 126p. ITC3 8202, (1982)

[2] **MONTOYA J.,** *Vibrations couplées de flexion et torsion d'une aube vrillée en rotation*. Revue Brown Boveri, Tome 53 N°3, pp216-230, (March 1966)

[3] **ISAKSON G., EISLEY J.G.,** *Natural frequencies in coupled bending and torsion of twisted rotating blades.* NASA Report, CR 65, NSG 27-59, (July 1964)

[4] **HODGES D.H., DOWELL E.H.,** *Nonlinear equations of motion for the elastic bending and torsion of twisted nonuniform rotor blade.* NASA Report Number: A-5711, NASA-TN-D-7818, (1974)

[5] **LALANNE M., FERRARIS-BESSO G.,** *Rotordynamics Prediction on Engineering.* John Wiley & Sons, 198p. ISBN : 0-471-92633-7, (1990)

[6] **VOLOVOI V., HODGES D.H.,** *Assessment of beam modeling methods for rotor blade applications.* Mathematical and computer modeling, ELSEVIER, vol 33, pp.1099-1112. ISSN : 0895-7177, (2001)

[7] **PRZEMIENIECKI J. S.,** *Theory of matrix structural analysis.* McGraw-Hill Book Company, New York, 480p. ISBN 0-486-64948-2, (1968)

[8] **YUNHUA L.,** *Explanation and elimination of shear locking and membrane locking with field consistence approach.* Computer methods in applied mechanics and engineering, ELSEVIER, pp249-269. ISSN : 0045-7825, (1998)

[9] **BATOZ J. L., DHATT G.,** *Modélisation des structures par éléments finis.* Edition Hermès, Paris, Vol 1 à 3. ISBN : 2-86601-259-3, (1990)

[10] **CRISFIELD M. A.,** *Non-linear finite element analysis of solids and structures*, Vol. 2, John Wiley & Sons, 508p. ISBN: 978-0-471-95649-5, (1997)

[11] **YU W., HODGES D.H., VOLOVOI V., CESNIK C.E.S.,** *On Timoshenko-like modeling of initially curved and twisted composite beams.* International journal of Solids and Structure, ELSEVIER, Vol 39, pp5101-5121. ISSN : 0020-7683, (2001)

[12] **CESNIK C.E.S., HODGES D.H., SUTYRIN V.G.,** *Cross-sectional analysis of composite beams including large initial twist and curvature effects.* AIAA Journal 34, 1913-1920, (1996)

[13] **HODGES D.H.,** *A review of composite rotor blade modeling.* AIAA Journal 28, 561-565. (1990)

[14] **BORRI M., MERLINI T.,** *Linear analysis of naturally curved and twisted anisotropic beams.* Composites Engineering 2, 433-456, (1992)

[15] **GERARDIN M., PETROV E.,** *Finite element theory for curved and twisted beams based on exact solutions for three-dimensional solids. Part1: Beam concept and geometrically exact nonlinear formulation.* Comput. Methods Appl. Mech. Engrg. 165, 43-92 (1998)

[16] **LIBRESCU L., SONG. O.,** *Thin-Walled composite beam.* Springer. ISBN : 1-420-3457-1, (2006)

[17] **CHANDRASHEKHARA K., KRISHNAMURTHY K., ROY S.,** *Free vibration of composite beams including rotary inertia and shear deformation*, Composite Structures 14 269-279, (1990),

[18] **MAHAPATRA D.R., GOPALAKRISHNAN S.,** *A spectral finite element model for analysis of axial-flexural-shear coupled wave propagation in laminate composite beams*, Composite Structures 59, 67-88, (2003)

[19] **BANERJEE J.R., GUO S., HOWSON W.P.,** *Exact dynamic stiffness matrix of a bending-torsion coupled beam including warping.* Computer & Structures Vol. 59, No. 4, pp. 613-621, (1996)

[20] **WITTRICK W.H., WILLIAMS F.W.,** *A general algorithm for computing natural frequencies of elastic structures*, Quarterly Journal of Mechanics and Applied Mathematics 24, 263-284, (1971)

[21] **TIMOSHENKO S., GOODIER J.N.,** *Theory of elasticity*. McGraw-Hill Book Co., (1934)

[22] **COWPER G.R.,** *The shear coefficient in Timoshenko's beam theory.* Journal of Applied Mechanics, (1966)

[23] **CRAIG Jr. R.R. , BAMPTON, M.C.C**., *Coupling of substructures for dynamic analysis*, AIAA Journal, July 1968, Vol. 6, N° 7, p.1313-1319